Geometry of Simple Molecules: Nonbonded Interactions, Not Bonding Orbitals, and Primarily Determine Observed Geometries

Ronald F. See,* Anthony D. Dutoi, Kevin W. McConnell, and Robert M. Naylor

Contribution from the Departments of Chemistry, Indiana University of Pennsylvania, Indiana, Pennsylvania 15705, and Saint Louis University, St. Louis, Missouri 63103

Received October 5, 2000. Revised Manuscript Received January 19, 2001

Abstract: The forces responsible for the observed geometries of the YX_3 (Y = N or P; X = H, F, or Cl) molecules were studied through ab initio computations at the HF-SCF/6-31G* level. The calculated molecular orbitals were grouped as contributing primarily to (a) the covalent bonds, (b) the terminal atom nonbonding electrons (for X = F or Cl), and (c) the central atom nonbonding electrons. This grouping was accomplished through 3-D plotting and an atomic population analysis of the molecular orbitals. The molecules were then moved through a X−Y−X angular range from 90° to 119°, in four or five degree increments. Single-point calculations were done at each increment, so as to quantify the energy changes in the molecular orbital groups as a function of geometry. These calculations show that the nonbonding electrons are much more sensitive to geometry change than are the bonding orbitals, particularly in the trihalide compounds. The molecular orbitals representing the nonbonding electrons on the terminal atoms (both valence and core electrons) contribute to the *spreading forces*, as they favor a wider X−Y−X angle. The *contracting forces*, which favor a smaller X−Y−X angle, consist of the orbitals comprising the nonbonding electrons on the central atom (again, both valence and core electrons). The observed geometry is seen as the balance point between these two sets of forces. A simple interaction-distance model of spreading and contracting forces supports this hypothesis. Highly linear trends are obtained for both the nitrogen trihalides ($R^2 = 0.981$) and phosphorus trihalides ($R^2 = 0.992$) when the opposing forces are plotted against each other. These results suggest that a revision of the popular conceptual models (hybridization and VSEPR) of molecular geometry might be appropriate.

Introduction

The approximate molecular geometry of main-group molecules is a fundamental piece of chemical knowledge. In fact, the need for conceptual models to determine molecular geometry is so well established that these models are included in virtually all introductory chemistry textbooks. The two models currently presented in this area are the hybridization, or directed valence, model[1−4] and the VSEPR, or electron domain, model.[5−9] The general precepts of both these models are far too familiar to require explanation, but a few points of importance should be noted. First, both models are based on a localized electron pair assumption, although each (to some extent) can be reconciled to the reality of delocalized molecular orbitals. Second, both models focus primarily on the electron pairs associated with the central atom, these being either bonding pairs or lone pairs of electrons. Finally, neither model has been quantitatively shown to be based on those physical forces primary responsible for observed molecular geometries. Debates between the two theories have instead focused on the relative predictive abilities and theoretical deficiencies of the respective models.[4,9,10]

Aside from any theoretical concerns, there are some observable anomalies when comparing analogous series of relatively simple compounds that are difficult to explain with either model. Among the most simple and striking of these are the trends in bond angle[10] and inversion barrier[10,11] among the trigonal pyramidal molecules of Group 15:

	X-Y-X degrees	ΔH_{inv} kJ/mol		X-Y-X degrees	ΔH_{inv} kJ/mol
NH_3	107.3(2)	24.5	PH_3	93.32(2)	155
NF_3	102.4(3)	~250	PF_3	96.7(7)	–
NCl_3	107.1(5)	–	PCl_3	100.1(3)	–

Of particular interest is the *decrease* in bond angle upon fluoridation of ammonia, while fluoridation of phosphine *increases* the bond angle.[12] Also problematic is the very large inversion energy for NF_3.[13] The deficiencies of both hybridization and VSEPR in explaining these trends were presented in

* Address correspondence to this author at Indiana University of Pennsylvania.

(1) Pauling, L. *The Nature of the Chemical Bond*; Cornell University Press: Ithaca, 1960.
(2) Landis, C. R.; Cleveland, T.; Firman, T. K. *J. Am. Chem. Soc.* **1995**, *117*, 1859.
(3) Landis, C. R. In *Advances in Molecular Structures*; Hargittai, I., Hargittai, M., Eds.; JAI Press: Greenwich, CT, 1996; Vol. 2, pp 129−161
(4) Cleveland, T.; Landis, C. R. *J. Am. Chem. Soc.* **1996**, *118*, 6020.
(5) Gillespie, R. J.; Nyholm, R. S. *Quart. Rev. (London)* **1957**, *11*, 339.
(6) Bader, R. F. W.; Gillespie, R. J.; MacDougall, P. J. *J. Am. Chem. Soc.* **1988**, *110*, 7329.
(7) Gillespie, R. J.; Hargittai, I. *The VSEPR Model of Molecular Geometry*; Allyn and Bacon: Boston, 1991.
(8) Gillespie, R. J. *Chem. Soc. Rev.* **1992**, 59.
(9) Gillespie, R. J.; Robinson, E. A. *Angew. Chem., Int. Ed. Engl.* **1996**, *35*, 495.
(10) Gilheany, D. C. *Chem. Rev.* **1994**, *94*, 1339.
(11) Bock, H.; Goebel, I.; Havlas, Z.; Liedle, S.; Oberhammer, H. *Angew. Chem., Int. Ed. Engl.* **1991**, *30*, 187.
(12) Massey, A. G. *Main Group Chemistry*; Ellis Horwood: London, 1990.

10.1021/ja003604b CCC: $20.00 © 2001 American Chemical Society
Published on Web 02/28/2001

depth by Gilheany;[10] we will only note here that both models require added postulates to explain the above data. Of course, there are other molecular systems, such as the bent CaX_2 molecules,[14,15] which are difficult to explain with either the hybridization or VSEPR models.[16] Gillespie and Robinson[17] recently suggested that the "traditional" VSEPR model may have substantial flaws, which may lead one to "unneccesarially complicated" descriptions of molecular bonding and geometry. Although ab initio calculations at a sufficiently high level can account for many of these appearently anomolous trends, the complexity of such calculations precludes them from serving as a compact, simple model of molecular geomerty. All of this suggests that it is time to refine our conceptual models of molecular geometry, so that they are consistent with both observed molecular geometries and the results of modern computational methods.

The hegemony of the two aforementioned models of molecular geometry may lead many to believe that there are no viable alternatives, or at least none that do not require extensive calculation. However, at least two other models have been proposed. One is based on perturbation theory, with the essential value being the relative magnitude of the HOMO-LUMO energy gap in the planar YX_3 molecule.[18] In early calculations, this model had shown promise in explaining the geometries of NH_3, PH_3, and possibily the triflourides,[19,20] and was included in Gilheany's more recent review article.[10] Another model is based on minimization of ligand nonbonded interactions, and is sometimes called the ligand close-packing (LCP) model. Bartell, who did much of the development of the LCP model, showed it to be very successful in predicting the geometry about atomic centers that lack nonbonding (lone pair) electrons.[21,22] While similar to VSEPR, the LCP model has an important difference: [23] VSEPR is based on the maximization of space for bonding pairs and lone pairs about the central atom, whereas the LCP model maximizes space for the atoms or groups bound to the atom of interest—the bonding electrons of the central atom were not considered to have a substantial effect on geometry. The LCP model had the additional advantage of being quantitative, and a good fit was obtained between observed and calculated bond angles for a variety of compounds.[21] Unfortunately, lone-pair electrons on the central atom were difficult to include in this model,[23] and possibly for this reason, the LCP model has fallen into relative obscurity (although it does seem to be enjoying a recent renaissance[17,24,25]).

As mentioned earlier, none of the available models has been quantitatively shown to be based on the physical forces responsible for molecular geometry. The ideal experiment would consist of recording the changes in energy of the various electronic features (covalent bonds, lone pairs on the central atom, lone pairs on terminal atoms, etc.) as a function of bond angle. The problem with such a computational experiment is the difficulty in assigning calculated molecular orbitals (MOs) to localized electronic features of a molecule. True molecular orbitals are delocalized over part or all of the molecule, so assignment of these orbitals to any particular atom or bond is often impossible.[26,27] Computational localization procedures,[28−30] while they do not change the energy of the sum of the MOs, do affect the energies of the individual orbitals, so their use in such an experiment introduces unwanted assumptions.

Given this difficult state of affairs, it is fortunate that there is one group of molecules—the trigonal pyramidal YX_3 molecules of Group 15—where an assignment of the true MOs to localized electronic features (a quasi-localization) may give useful results. The quasi-localization of these molecules is based on three factors: (1) there is only one lone pair on the central atom; (2) there are no multiple bonds; (3) in the fluorinated and chlorinated molecules, the central atom is usually less electronegative than the terminal atoms. Of course, the expectation is that the MOs assigned to any localized electronic feature will be delocalized over all atoms which share that feature, but this is not a detriment to such an analysis. The only necessary data are the energetic change of the *group* of MOs assigned to that feature, as a function of geometry change.

Any quasi-localization, such as described above, requires substantiation, and there are two techniques that may be useful in this regard: visualization of the molecular orbital and an atomic population analysis of the MO. The atomic population analysis gives the fraction of the electron density of the individual MO in the region of each atom. For instance, the MO assigned as the lone pair on the central atom should have a high atomic population in the region of that (N or P) atom, and a low population in the region of the terminal atoms. If the quasi-localization scheme can be validated by the above techniques, it would be a useful method for determining the origins of the physical forces most responsible for the observed geometry of these trigonal pyramidal YX_3 molecules. Additionally, although this technique is probably not generally applicable to other molecular types, the conclusions from this study may help us understand the basis of geometry in all simple main-group molecules.

Computational Details

All computations were done on a PC, running either the MacSpartan Pro or Titan program packages.[31] The equilibrium geometry of each molecule was determined by geometry optimization at the HF-SCF/6-31G* level, and the MO visualizations were produced from these structures. The primary protocol (fixed-distance) for the fixed-geometry calculations was as follows: (a) bond distances fixed at the geometry-

(13) Schwerdtfeger, P.; Hunt, P. In *Advances in Molecular Structure Research*; Hargittai, M., Hargittai, I., Eds.; JAI Press: Greenwich, CT, 1999; Vol. 5, p 223.
(14) Hargittai, M. In *Stereochemical Applications of Gas-Phase Electron Diffraction*; Hargittai, I., Hargittai, M., Eds.; VCH: New York, 1988; Vol. B, p 383.
(15) Hargittai, M.; Hargittai, I. In *Structures and Conformations of Non-Rigid Molecules*; Laane, J., Dakkouri, M., Van der Veken, B., Oberhammer, H., Eds.; NATO ASI Series C: Mathematical and Physical Sciences, Vol. 410; Kluwer: Dordrecht, The Netherlands, 1993.
(16) Bytheway, I.; Gillespie, R. J.; Tang, T.-H.; Bader, R. F. W. *Inorg. Chem.* **1995**, *34*, 2407.
(17) Gillespie, R. J.; Robinson, E. A. In *Advances in Molecular Structures*; Hargittai, I., Hargittai, M., Eds.; JAI Press: Greenwich, CT, 1998; Vol. 4, pp 1−41.
(18) Pearson, R. *J. Am. Chem. Soc.* **1969**, *91*, 4947.
(19) Cherry, W. R.; Epiotis, N. D. *J. Am. Chem. Soc.* **1976**, *98*, 1135.
(20) Cherry, W. R.; Epiotis, N. D.; Borden, W. T. *Acc. Chem. Res.* **1977**, *10*, 167.
(21) Bartell, L. S. *J. Chem. Phys.* **1960**, *32*, 827.
(22) Bartell, L. S. *Tetrahedron* **1962**, *17*, 177.
(23) Bartell, L. S. *J. Chem. Educ.* **1968**, *45*, 754.
(24) Gillespie, R. J. *Coord. Chem. Rev.* **2000**, *197*, 51.
(25) Levy, J. B.; Hargittai, I. *J. Mol. Struct. (THEOCHEM)* **1998**, *454*, 127.
(26) Albright, T. A.; Burdett, J. K.; Whangbo, M.-H. *Orbital Interactions in Chemistry*; Wiley: New York, 1985.
(27) Burdett, J. K. *Chemical Bonds: A Dialogue*; Wiley: Chichester, 1997.
(28) Boys, S. F. In *Quantum Theory of Atoms, Molecules and the Solid State*; Lowdin, P. O., Ed.; Academic Press: New York, 1966; p 253.
(29) Edminson, C.; Reudenberg, K. In *Quantum Theory of Atoms, Molecules and the Solid State*; Lowdin, P. O., Ed.; Academic Press: New York, 1966; p 263.
(30) Reed, A. E.; Curtiss, L. A.; Weinhold, F. *Chem. Rev.* **1988**, *88*, 899.
(31) *MacSpartan Pro: Tutorial and User's Guide*; Wavefunction, Inc.: Irvine, CA, 1998.

Table 1. Observed and Computed[a] Structural Data for the YX_3 Molecules

	X−Y−X, deg		Y−X, Å		X−X, Å			VdWr overlap, Å	
YX_3	obsd	calcd	obsd	calcd	obsd	calcd	VdWr, X	obs	calcd
NH_3	107.3(2)	107.2	1.008(4)	1.003	1.63	1.62	1.20	0.77	0.76
NF_3	102.4(3)	102.7	1.365(2)	1.328	2.13	2.07	1.55	0.97	1.03
NCl_3	107.1(5)	110.2	1.759(4)	1.722	2.83	2.83	1.80	0.77	0.77
NBr_3		114.3		1.900		3.19	1.90		0.61
NI_3		120.0		2.051		3.55	2.03		0.51
PH_3	93.32(2)	95.5	1.412(1)	1.403	2.05	2.08	1.20	0.35	0.32
PF_3	96.7(7)	97.3	1.563(2)	1.564	2.34	2.35	1.55	0.76	0.75
PCl_3	100.1(3)	100.9	2.043(1)	2.047	3.13	3.16	1.80	0.47	0.44
PBr_3	98.8(3)	101.2	2.220(3)	2.220	3.43	3.51	1.90	0.37	0.29
PI_3		102.9		2.529		3.95	2.03		0.11

[a] HF-SCF 6-31G* for X = H, F, or Cl and 3-21G* for X = Br or I.

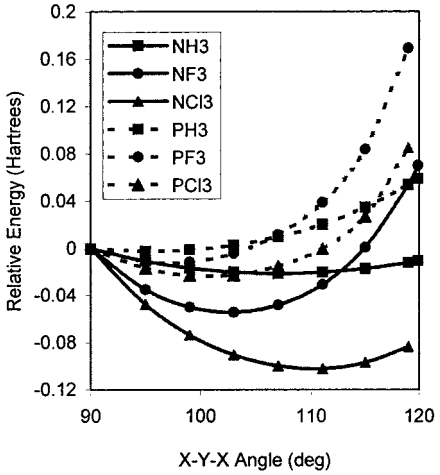

Figure 1. Calculated total relative energy of the YX_3 molecules. All computations at the HF-SCF/6-31G* level.

optimized values; (b) bond angles set equal, and at the values 90°, 95°, 99°, 103°, 107°, 111°, 115°, and 119°; (c) single-point calculations done, also at the HF/6-31G* level; and (d) MO energies and visualizations taken directly from the computational output, without manipulation. To ensure that the conclusions of this study were not method-dependent, an additional set of calculations were done (HF/6-31G*) where the X−Y−X angle was fixed, but the Y−X distance was allowed to refine (refined-distance protocol). Finally, to demonstrate the adequacy of the HF/6-31G* calculation for phosphorus compounds,[25] fixed-geometry calculations on PF_3 were also carried out at the LMP2/6-31G** level.

Atomic occupancy of the calculated MOs was taken from the geometry-optimized structures. The atomic populations were calculated by squaring the coefficients of the atomic orbital functions included in the MO, then summing these values for each atomic orbital function associated with that atom and dividing by the sum of squares of all atomic orbital functions in the MO.

Results

Prediction of Equilibrium Geometries and Inversion Barriers. The HF/6-31G* calculations adequately predict the observed geometries of the YX_3 molecules.[25] Table 1 gives the observed and predicted bond distances and angles for the YX_3 molecules. Figure 1 shows the total calculated relative energies of these molecules in the X−Y−X range from 90° to 119°. The minimum of each curve is the predicted equilibrium structure. The energy difference from this minimum to the energy at X−Y−X = 120° approximates the predicted inversion barriers, which are as follows (in kJ/mol, with experimental value in parentheses, if known[10,11]): NH_3 = 28 (24.5), NF_3 = 320 (~250), NCl_3 = 51, PH_3 = 160 (155), PF_3 = 440, and PCl_3 = 280. These calculated inversion barriers also show good agreement with the known values.

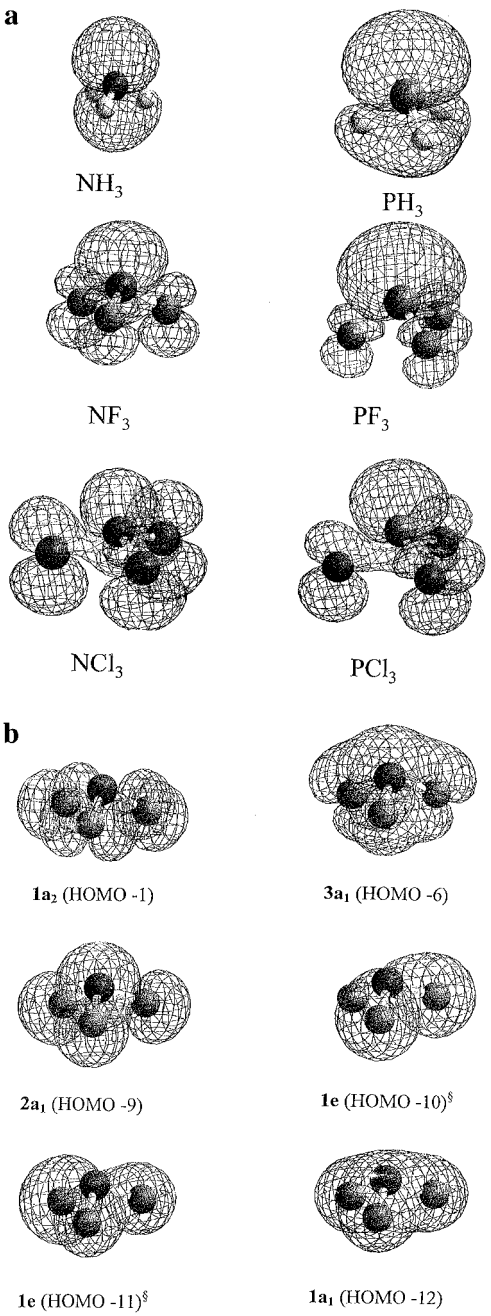

Figure 2. Selected molecular orbitals of the YX_3 molecules: (A) highest occupied molecular orbitals (HOMO) and (B) selected orbitals of NF_3.

Validation of the Quasi-localization Scheme. Figure 2 gives the selected MO visualizations from the YX_3 molecules,

Table 2. Fractional Atomic Populations[a] and Energies of Calculated Molecular Orbitals in YX_3 Molecules

orbital	NH_3 N/H	NF_3 N/F	NCl_3 N/Cl	PH_3 P/H	PF_3 P/F	PCl_3 P/Cl
fractional atomic populations by valence molecular orbital						
4 A_1		0.587 / 0.138	0.389 / 0.204		0.701 / 0.100	0.516 / 0.161
1 A_2		0.000 / 0.333	0.000 / 0.333		0.000 / 0.333	0.000 / 0.333
4 E		0.022 / 0.326	0.020 / 0.327		0.030 / 0.323	0.013 / 0.329
3 E		0.021 / 0.326	0.023 / 0.326		0.030 / 0.323	0.017 / 0.328
3 A_1		0.282 / 0.239	0.459 / 0.180		0.156 / 0.281	0.262 / 0.246
2 E		0.197 / 0.268	0.296 / 0.235		0.151 / 0.283	0.207 / 0.264
2 A_1	0.972 / 0.009	0.364 / 0.212	0.302 / 0.233	0.910 / 0.030	0.325 / 0.225	0.435 / 0.188
1 E	0.662 / 0.113	0.036 / 0.321	0.045 / 0.318	0.455 / 0.182	0.015 / 0.328	0.027 / 0.324
1 A_1	0.875 / 0.042	0.153 / 0.282	0.491 / 0.170	0.862 / 0.046	0.056 / 0.315	0.147 / 0.284
fractional atomic populations by quasi-localization feature						
central lone pair	0.972 / 0.009	0.587 / 0.138	0.389 / 0.204	0.910 / 0.030	0.701 / 0.100	0.516 / 0.161
terminal lone pairs		0.017 / 0.328	0.091 / 0.303		0.024 / 0.325	0.012 / 0.329
bonding orbitals	0.733 / 0.089	0.075 / 0.308	0.194 / 0.269	0.590 / 0.137	0.029 / 0.324	0.067 / 0.311
terminal core		0.000 / 0.333	0.000 / 0.333		0.000 / 0.333	0.000 / 0.333
central core	1.0 / 0.0	1.0 / 0.0	1.0 / 0.0	1.0 / 0.0	1.0 / 0.0	1.0 / 0.0
overall energy (hartrees)						
MacSpartan Pro	−56.184356	−352.540057	−1432.735511	−342.447959	−639.129229	−1719.213494
orbital energies (hartrees)						
4 A_1		−0.535	−0.414		−0.452	−0.408
1 A_2		−0.671	−0.465		−0.640	−0.472
4 E		−0.678	−0.482		−0.653	−0.483
3 E		−0.739	−0.521		−0.696	−0.523
3 A_1		−0.855	−0.651		−0.748	−0.582
2 E		−0.863	−0.667		−0.764	−0.614
2 A_1	−0.420	−1.108	−0.928	−0.383	−0.892	−0.812
1 E	−0.628	−1.663	−1.137	−0.529	−1.618	−1.126
1 A_1	−1.140	−1.821	−1.357	−0.860	−1.680	−1.206
HOMO−LUMO gap (hartrees)						
planar YX_3	0.6050	0.5609	0.3989	0.4529	0.2565	0.2572

[a] Values listed are for *each* atom. Therefore, total occupancy of a MO = (occupancy at central atom) + (3 × occupancy at terminal atom).

including the HOMO ($2a_1$ for NH_3 and PH_3, $4a_1$ for others) for all six molecules studied; the complete set of these visualizations has been deposited in the Supporting Information. It is visually clear from Figure 2 that, in each case, the HOMO is very strongly associated with the nonbonding (lone) electron pair on the central atom. For comparison, the next-lowest-energy ($1a_2$) MO of NF_3 can be seen to have insignificant electron density on the central (nitrogen) atom; the $1a_2$ MOs of NCl_3, PF_3, and PCl_3 are virtually identical. Further evidence of the strong association of the HOMO with the central atom lone pair is given by the $1a_1$, 1e, and $2a_1$ MOs of NF_3, which have significant populations about the nitrogen atom (see below and Table 2). However, the visualizations show that these MOs are not in the correct spatial domain to contribute significantly to the central atom lone pair, and are better assigned as bonding MOs (see below).

To provide a more quantitative validation of the quasi-localization scheme, fractional atomic populations of the molecular orbitals were calculated; the results of these calculations are given in Table 2. Of particular interest are the values for the HOMOs and, for the fluorinated and chlorinated molecules, the orbitals directly following the HOMO ($1a_2$ to $2a_1$). With one exception, the HOMOs show a very substantial fraction of their population in the region of the central atom, and this fraction is larger than that for any other molecular orbital. The one exception, NCl_3, is no surprise. Nitrogen and chlorine are a close match in electronegativity, so it is expected that the nonbonding MOs would be more equal in energy, and show considerable mixing. The identification of the HOMO with the central atom lone pair is obvious for NH_3 and PH_3, and for the other three molecules (NF_3, PF_3, and PCl_3), the central atom is clearly less electronegative than the terminal atoms. It follows that the nonbonding electrons associated with the central atom would be expected to be in a higher energy MO than those associated with the terminal atoms. Therefore, by MO visualization, atomic population analysis, and theoretical arguments, it is valid to associate the central atom lone pair with the HOMO for at least five of the six molecules studied.

If the HOMO can generally be associated with the lone pair on the central atom, then the quasi-localization for NH_3 and PH_3 is clear, with the three lower energy MOs associated with the covalent bonds. The population analysis in Table 2 and the MO visualizations support this interpretation.

For the fluorinated and chlorinated molecules, the assignments are significantly more complex. A possible expectation is that the nine MOs below the HOMO should be associated with the lone pairs of the fluorine or chlorine atoms, and the three lowest energy valence MOs should be associated with the covalent bonds. However, the reality of delocalized molecular orbitals is that very significant mixing will take place when this many valence electrons are involved. A close inspection of Table 2 yields the following trends: (A) The orbitals $1a_2$, 4e, and 3e (HOMO-1 to HOMO-5) are very strongly associated with the lone pairs on the terminal atoms. For these five orbitals, the population on the central atom averages only 1.75% for all four compounds, and never is it higher than 3.0% (4e and 3e of PF_3). The orbital visualization also shows these orbitals to be in the correct spatial domain for terminal atom lone pairs. (B) The orbitals $3a_1$, 2e, and $2a_1$ (HOMO-6 to HOMO-9) are too delocalized to be associated with any localized electronic feature of the molecule. The average central/terminal population ratio for these four orbitals, for the fluorinated and chlorinated compounds, is 0.268/0.244. The visualization of these MOs shows that, while there may be some bonding character to these orbitals, they are in the wrong spatial domain to be the orbitals primary associated with the covalent bonds. (C) The orbitals 1e and $1a_1$ (HOMO-10 to HOMO-12) are strongly associated with the covalent bonds. These orbitals *are* in the correct spatial

Table 3. Relative Energies (in hartrees, fixed-distance protocol) of Quasi-localization Features as a Function of Geometry: YH_3, YF_3, and YCl_3 Compounds

(a) YH_3 Compounds

angle	central core	covalent bonds	central lone pair	angle	central core	covalent bonds	central lone pair
NH_3				**PH_3**			
90	0	0	0	90	0	0	0
95	0.00427	−0.00358	0.01592	95	−0.00072	−0.01831	0.01403
99	0.00785	−0.0061	0.02871	99	−0.00136	−0.0323	0.02576
103	0.01162	−0.00802	0.04156	103	−0.00197	−0.04542	0.03807
107	0.01566	−0.00906	0.05447	107	−0.00232	−0.05725	0.05108
111	0.02002	−0.00893	0.06742	111	−0.00227	−0.06732	0.06491
115	0.02479	−0.00727	0.08038	115	−0.00166	−0.07488	0.0796
119	0.03003	−0.00375	0.09327	119	−0.00083	−0.07885	0.09503

(b) YF_3 and YCl_3 Compounds

X−Y−X angle	central core	terminal cores	covalent bonds	undefined orbitals	terminal lone pairs	central lone pair
NF_3						
90	0	0	0	0	0	0
95	0.0033	−0.0272	−0.00784	−0.00062	−0.05568	0.01952
99	0.00799	−0.04619	−0.0133	−0.00076	−0.09309	0.03636
103	0.015	−0.06307	−0.01726	0.00052	−0.12493	0.05501
107	0.02524	−0.07789	−0.0188	0.0046	−0.15131	0.07633
111	0.04046	−0.09067	−0.01646	0.01367	−0.17207	0.10151
115	0.06493	−0.10144	−0.00728	0.0325	−0.18632	0.13235
119	0.11074	−0.10912	0.01765	0.07527	−0.19053	0.17076
NCl_3						
90	0	0	0	0	0	0
95	0.00196	−0.03655	0.00989	0.01709	0.00753	−0.01215
99	0.00496	−0.06359	0.01663	0.02907	0.0142	−0.02021
103	0.00961	−0.08892	0.02332	0.04063	0.00643	−0.01155
107	0.01643	−0.11323	0.03081	0.0528	−0.00441	0.0028
111	0.02625	−0.13764	0.04023	0.06678	−0.01254	0.0176
115	0.04072	−0.16434	0.05316	0.08437	−0.01779	0.03347
119	0.06334	−0.19751	0.07287	0.10919	−0.01959	0.05106
PF_3						
90	0	0	0	0	0	0
95	0.00396	−0.03658	−0.02729	−0.02138	−0.06952	0.01659
99	0.00759	−0.06236	−0.04709	−0.03742	−0.11742	0.03187
103	0.01137	−0.0848	−0.06446	−0.05162	−0.15834	0.04947
107	0.01459	−0.1034	−0.07868	−0.06304	−0.19166	0.07011
111	0.01588	−0.11708	−0.08868	−0.07037	−0.21574	0.09504
115	0.01055	−0.12206	−0.09164	−0.07068	−0.22484	0.12684
119	−0.05676	−0.07886	−0.06344	−0.0427	−0.1654	0.16482
PCl_3						
90	0	0	0	0	0	0
95	0.01192	−0.08076	−0.00713	−0.0007	−0.03619	0.01261
99	0.02337	−0.13866	−0.0127	−0.00164	−0.06104	0.02344
103	0.03647	−0.19139	−0.01785	−0.00245	−0.08264	0.03549
107	0.05163	−0.23908	−0.02216	−0.00266	−0.1011	0.04946
111	0.07011	−0.28152	−0.02506	−0.00142	−0.11608	0.06645
115	0.0964	−0.31923	−0.02537	0.00304	−0.12686	0.08888
119	0.17531	−0.39121	−0.01886	0.02218	−0.13559	0.12745

domain for covalent bonds, and the low energy of these orbitals (in particular the energy drop from the 2e to 1e orbitals) suggests that these orbitals have strong bonding character. On the basis of the above, the final quasi-localization scheme for the YH_3 and YX_3 molecules is given in Figure 3.

The nonassignment of orbitals $3a_1$, 2e, and $2a_1$ is, in some ways, an advantage in this analysis. In effect, they act as a barrier between the bonding and nonbonding orbitals. While it is reasonable to suggest that there is significant bonding character to the $2a_1$ and 2e orbitals, the 3e orbitals (the lowest energy orbitals strongly associated with lone pairs) are simply too high in energy, and in the wrong spatial domain, to make a significant contribution to the covalent bonds. The fact that the $3a_1$, 2e, and $2a_1$ orbitals are, as a group, very insensitive to changes in molecular geometry (see below) makes their assignment even less of an issue, as their inclusion (or noninclusion) in either group would have no significant effect on the conclusions of this study.

Energy Changes in the Localized Electronic Features as a Function of Bond Angle. Since the change in energy, as a function of geometry change, was the focus of these calculations, energy relative to a X−Y−X bond angle of 90° gives the clearest indication of these trends. The relative energy is given by the following:

$$\mathrm{RE_X} = \sum\nolimits_{\mathrm{X}} (E_{\mathrm{MO}}(\theta) - E_{\mathrm{MO}}(90°))$$

Where RE_X is the relative energy of the localized electronic feature (i.e., the quasi-localization groups) X, $\sum_x$ is the summation of the MOs grouped in the localized electronic feature X, $E_{MO}(\theta)$ is the energy eigenvalue for the molecular orbital at

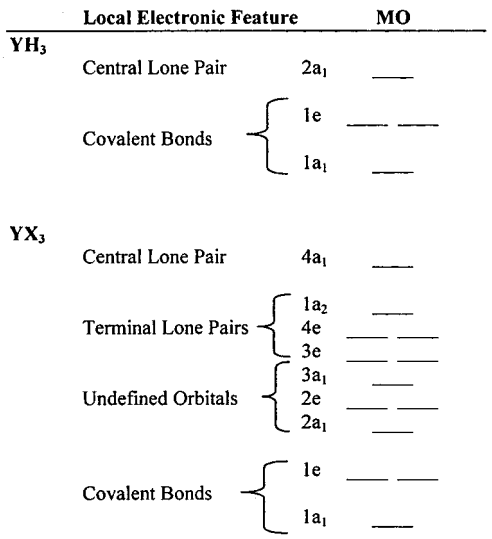

Figure 3. Proposed quasi-localization scheme for YX_3 molecules.

angle θ, and $E_{MO}(90°)$ is eigenvalue for the molecular orbital at 90°. The energetic data for the localized electronic features, as a function of X−Y−X bond angle, is given in Table 3, parts a (for YH_3) and b (for YF_3 and YCl_3), for the fixed-distance protocol (analogous data for the refined-distance protocol are collected in the Supporting Information). Since the quasi-localization procedure is not legitimate for NCl_3, the energy values for the noncore features of NCl_3 have little meaning, but have been provided for completeness. Plots of the X−Y−X angle versus relative energy for the molecules studied (omitting NCl_3) are given in Figure 4, for both the fixed- and refined-distance protocols. The suitability of the HF/6-31G* computation for these molecules is demonstrated by Figure 5, where fixed-geometry calculations (refined-distance protocol) at both the LMP2/6-31G** and HF/6-31G* levels are presented. It can be seen that only a slight difference in magnitude, and absolutely no difference in trend, can be observed between these two calculations.

The trends apparent from the fixed-geometry calculations may be divided into three groups: (1) the effect of geometry change on the lone pair orbitals; (2) the surprising sensitivity of core orbitals to changes in geometry; and (3) the relative insensitivity of the covalent bonds to geometry.

(a) Effect of Geometry Change on Lone Pair Orbitals.

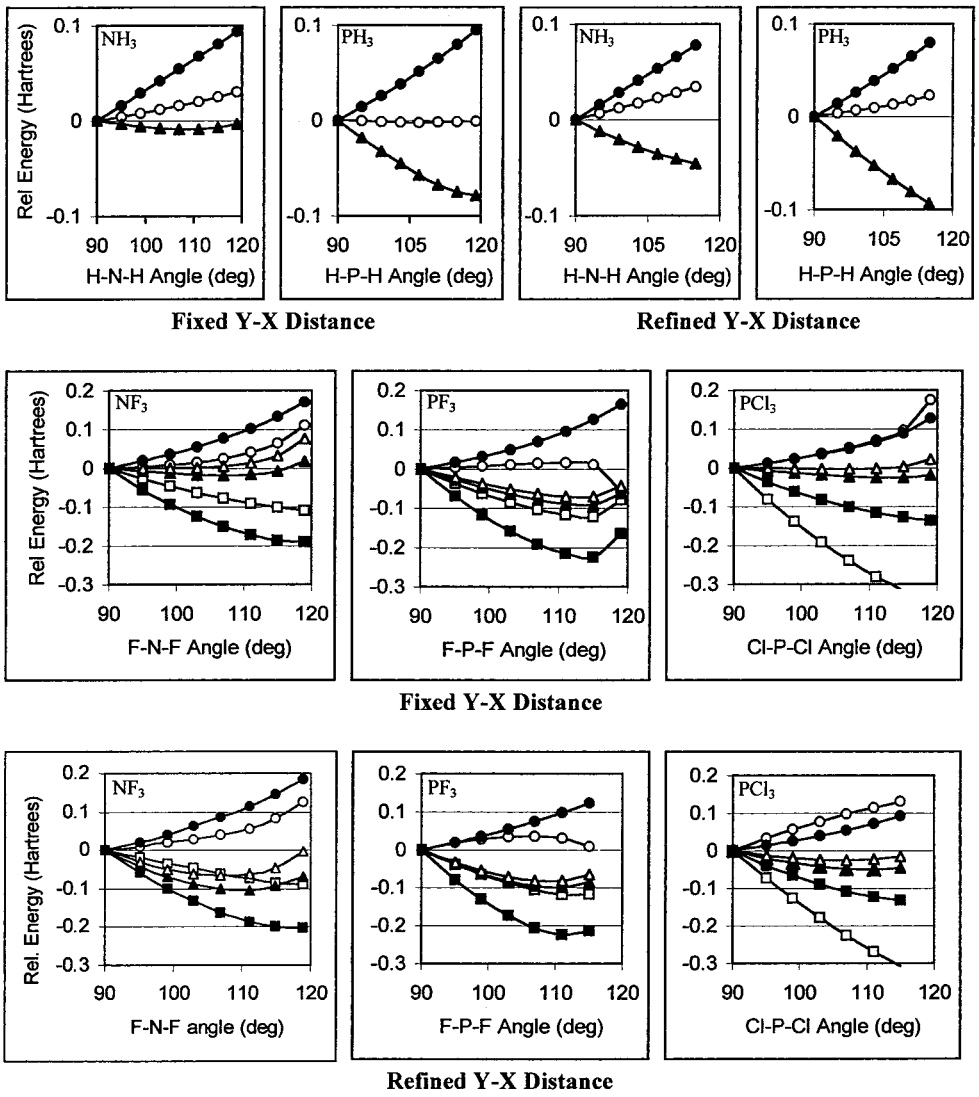

Figure 4. Modified Walsh diagrams of the YX_3 molecules, using both the fixed- and refined-distance protocols. Quasi-localization groups are indicated as follows: central atom core orbitals = open circles (○); terminal atom core orbitals = open squares (□); covalent bonds = filled triangles (▲); undefined orbitals = open triangles (△); terminal atom nonbonding electrons (lone pairs) = filled squares (■); central atom nonbonding electrons (lone pair) = filled circles (●).

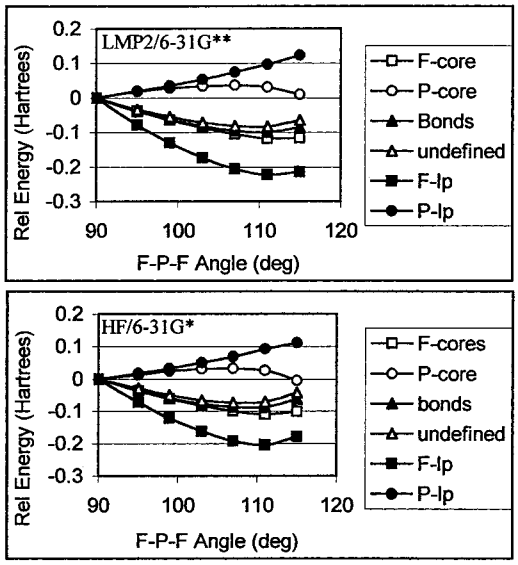

Figure 5. Modified Walsh diagrams (refined-bond protocol) of PF_3 at the LMP2/6-31G** and HF/6-31G* levels.

Figure 4 shows that, for all molecules, the lone pair orbitals are very sensitive to geometry changes. The central atom lone pair always favors a smaller X−Y−X angle, while in the trihalides, the halide-atom lone pairs favor angles larger than the observed geometries. In all the YX_3 molecules except PCl_3, the lone pair orbitals are the most sensitive quasi-localization group to geometry change. In PCl_3, the sensitivity of the lone pair orbitals is equaled or surpassed by the sensitivity of the phosphorus and chlorine core orbitals.

(b) Sensitivity of the Core Orbitals to Changes in Geometry. It would come as no surprise that the lone pair of NH_3 would increase in energy as the geometry of the molecule moves from pyramidal to planar (i.e., 90° to 120°). However, it is somewhat less expected that the energy of the core 1s electrons should change significantly in this angular range. The energy of the 1s core in NH_3 increases with increasing angle. The magnitude of this energy change from the observed H−N−H angle of 107.5° to 119° is 0.01437 hartrees (37.7 kJ/mol); this must be considered significant as it is ∼50% larger than the predicted thermodynamic inversion barrier (28 kJ/mol) for NH_3. This trend appears to be quite general, only PH_3 (fixed-distance protocol) shows core orbitals essentially insensitive to angular changes.

In the YF_3 and YCl_3 molecules, the core orbitals of the fluorine and chlorine atoms are also surprisingly sensitive to angular changes. The trend here is opposite that of the central cores, in that the energy decreases as angle increases toward 120°. Again, the magnitude of these changes is very significant. For NF_3 (which has the smallest changes of the four molecules studied), the change in the energy of the fluorine cores from the observed geometry (102.5°) to 119° is about 130 kJ/mol. The effect is most apparent in PCl_3, where the chlorine core orbitals show a higher sensitivity to geometry change than any other quasi-localization group in this study.

(c) Insensitivity of the Covalent Bonds to Geometry. For NH_3, NF_3, PF_3, and PCl_3 (fixed-distance protocol) the energy of those orbitals associated with the covalent bonds changes little with geometry. While the energy trends go through minima for all of these molecules, as might be expected from hybridization theory, these minima are shallow (compared to the changes in energy of the lone pairs) and usually at the wrong angle. The location and depth (relative to 90°) of these minima are as follows: NH_3 108°, 24 kJ/mol; NF_3 106°, 50 kJ/mol; PF_3 114°, 250 kJ/mol; and PCl_3 113°, 66 kJ/mol. For comparison, the changes in the energies of the terminal lone pairs (which have similar trends), relative to 90°, are 500 kJ/mol for NF_3, 590 kJ/mol for PF_3, and 360 kJ/mol for PCl_3. These values clearly show that any angular preference of the bonding orbitals can only make a minor contribution to the observed geometry, particularly for the YF_3 and YCl_3 molecules. The refined-distance protocol results in somewhat greater sensitivity of the bonding orbitals, but this sensitivity is still markedly less than that of the terminal-atom lone pair orbitals.

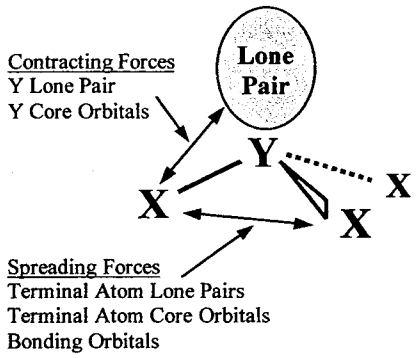

Figure 6. Diagram of the spreading and contracting forces in the YX_3 molecules.

The bonding orbitals in PH_3 show an energy change of 207 kJ/mol (fixed-distance) from 90°, but only go through a minimum at 120°. Since the observed bond angle for PH_3 is the most acute of the six molecules studied (94.3°), it is equally clear for this molecule that the angular preference of the bonding orbitals does not determine the observed geometry.

Discussion

Grouping of Features into Contracting and Spreading Forces. From the preceding discussion, as well as Figure 4, a picture of two sets of forces begins to emerge. One set may be termed *spreading forces*, and favors a more planar geometry, while an opposing set of forces, *contracting forces*, tend toward a more pyramidal geometry. An illustration of these two sets of forces is given in Figure 6.

The features grouped in the spreading forces include the nonbonding (lone pair) electrons on the terminal atoms and the core electrons of the terminal atoms. As the X−Y−X angle increases from 90°, the terminal atoms move further apart, and the energy of these features decreases. This trend continues through the observed X−Y−X angle in each molecule. The YF_3 molecules do show a dramatic increase in the energy of these features at angles approaching trigonal planar, which is probably due to the terminal lone pairs interacting more strongly with the central lone pair than with each other (notice, for example, that this inflection is not apparent for PCl_3, where the Y−X bond distance is much longer). The bonding orbitals also favor a larger X−Y−X angle, but may only be considered a minor contributor to the overall spreading forces, except in NH_3 and PH_3. Missing from this analysis, but a possible contributor to the spreading forces, are the internuclear repulsions between the terminal atoms. This energy must be important for NH_3 and may not be insignificant for the other molecules. However, since the quantification of this energy would not change the conclusions of this paper, it has not been included in the present work.

The contracting forces, features that favor a smaller X−Y−X angle, are the lone pair on the central atom and the core electrons on the central atom. It is not surprising that the lone pair of the

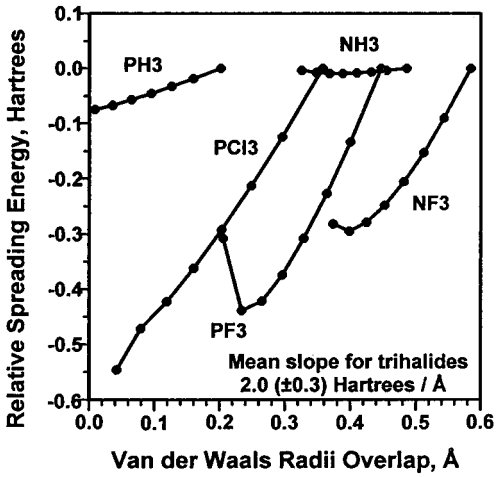

Figure 7. Correlation of spreading orbital energies with van der Waals radii overlap.

central atom favors a more contracted geometry, as larger X−Y−X angles bring the terminal atoms closer to the region of this feature. It is somewhat less obvious why the core electrons of the central atom should also favor smaller X−Y−X angles, but this observation has some interesting ramifications (see below). For the YH_3 and YF_3 molecules, the central lone pair is much more sensitive to geometric changes than are the core electrons of the central atom, but in PCl_3, these two features show approximately equal energetic changes.

Thus a model emerges of two competing sets of forces: one (the spreading forces) trying to make the molecule planar, and the other (the contracting forces) driving the X−Y−X bond angle toward smaller values. For the trihalide molecules, both groups are dominated by interactions between nonbonding electrons: the repulsive interaction between lone pairs and core electrons on terminal atoms for the spreading forces and the repulsive interaction between the central and terminal lone pairs and core electrons for contracting forces. The observed geometry is achieved when these two sets of forces are in equilibrium.

Modeling the Spreading Forces by van der Waals Radii Overlap. Unfortunately, while the concept of this model is straightforward, the variables of X−Y bond distance, X−Y−X angle, and terminal atom size complicate the application of the model. One way to simplify this problem is to explore the van der Waals radii[32] (VdWr) overlap of the terminal atoms. While VdWr is clearly an approximate measurement, the advantage of using the VdWr overlap is that X−Y−X angle, X−Y distance, and atomic size information are expressed in one value. The VdWr overlap as a function of X−Y−X angle can be calculated:

$$r_{\mathrm{VdW}}\ \mathrm{overlap} = 2[r_{\mathrm{VdW}} - \{\sin(\theta_{xyx}/2)\mathrm{d}_{xy}\}]$$

where r_{VdW} = van der Waals radii (Å), θ_{xyx} = X−Y−X angle (deg), and d_{xy} = X−Y bond distance (Å). To determine if the VdWr overlap is a valid model for the total spreading energies, the sum of the relative spreading energies (fixed-distance protocol) versus VdWr overlap was plotted. As can be seen in Figure 7, the plots for NF_3, PH_3, PF_3, and PCl_3 are highly linear (mean $R^2 = 0.994$) from 90° to 111°, a range that includes all of the observed geometries of these molecules. Thus it appears that the VdWr overlap model is a valid simplification of the total spreading energies. It should be noted that the three trihalides in Figure 7 have similar slopes, the mean value for these slopes being 2.0 ± 0.3 hartrees/Å. Were these spreading energies the product of simple columbic repulsion, such a slope would correspond to a point charge of 1.06 atomic charge units on each of the halide atoms, a value that seems too large, and certainly exceeds the calculated atomic point charges (electrostatic fit model) for these atoms. This underlines the point made by Bader and Gillespie[6,9,33] that while the repulsions between electron domains may act like columbic repulsions, the physical basis for these repulsions is much more complex.

The VdWr overlap of all the YX_3 molecules (including YBr_3 and YI_3 species) is given in Table 1. Unlike the angles presented in this table, the VdWr overlaps show a clear trend between the NX_3 molecules and their PX_3 analogues. In both series, the overlap increases from YH_3 to YF_3, and then decreases steadily from YF_3 to YI_3. These trends are consistent with the idea of a balance of spreading and contracting forces. In the YF_3 molecules, the short (relative to the other halides) Y−F bond results in greater interaction between the nonbonding electrons on the fluorine and those on the central atom, which yield relatively greater contracting forces. To balance these large contracting forces, we observe larger VdWr overlaps for the YF_3 molecules. As one progresses down the halides from fluorine to iodine, the Y−X distances get progressively longer, and so the total contracting forces would be progressively weaker. To balance these weakening contracting forces, progressively less VdWr overlap is "needed", and so the trend from YF_3 to YI_3 in Table 1 is as expected. The small VdWr overlap for the YH_3 species is also expected: because hydrogen lacks lone pairs, its repulsive interaction with the lone pair of the central atom is greatly reduced, so less VdWr overlap is required as balance. This model also explains the large inversion barrier in NF_3. The repulsive interaction between the nonbonding electrons on nitrogen and fluorine is large, and moving to a trigonal planar geometry increases this repulsion. NH_3 lacks nonbonding electrons on terminal atoms, so the increase in repulsive interaction upon moving toward planar geometry is much less than in NF_3.

While the VdWr overlap model gives a simple, reasonably accurate model for the interaction of the nonbonding electrons between terminal atoms, a correspondingly simple model for the interaction of nonbonding electrons between the central and terminal atoms is more difficult to envision. The location and radial extent of the central atom lone pair is not easy to quantify, and these values may change with the electronic nature of the terminal groups. However, if it is assumed that a columbic repulsion model will give an accurate representation of the contracting forces, then the relative magnitude of these forces will roughly scale with the Y−X bond distance; a plot of VdWr overlap (spreading forces) versus X−Y distance (contracting forces) is given in Figure 8. In this plot, R^2 is 0.981 for the nitrogen trihalides (two observed points, four calculated points) and 0.992 for the phosphorus trihalides (three observed points, four calculated points). The high linearity of these plots supports the validity of the concept that observed geometry is the geometry where a balance is achieved between spreading and contracting forces; this is especially true when one considers the bond angles in the equilibrium geometries range from 96.7° (observed structure of PF_3) to 120° (calculated structure of NI_3). Given the strong agreement of the data, the small difference between the nitrogen and phosphorus trihalides is probably significant, and it is also as expected. Nitrogen, being more electronegative than phosphorus, should have a higher charge density in the region of the central atom. This would lead to

(32) Bondi, A. *J. Phys. Chem.* **1964**, *68*, 441.

(33) Bader, R. F. W. *Atoms in Molecules: A Quantum Theory*; Clarendon Press: Oxford, 1990.

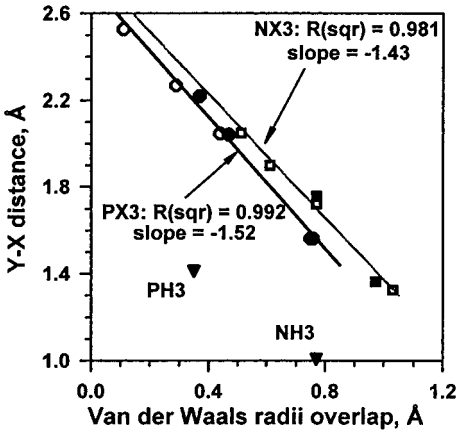

Figure 8. The balance of spreading orbital energies (as modeled by van der Waals radii overlap) and contracting orbital energies (as modeled by Y−X distance). The nitrogen trihalides are indicated by squares, the phosphorus trihalides by circles, and the YH_3 molecules by triangles. Filled symbols indicate observed structural data, while open symbols denote computed values.

greater contracting forces in the nitrogen compounds, relative to phosphorus compounds, for the same Y−X distance, and therefore require more VdWr overlap to balance these larger contracting forces. The outlier nature of NH_3 and PH_3 is also as expected. As mentioned above, the lack of nonbonding electrons on hydrogen greatly reduces the terminal atom−central atom repulsive interactions (contracting forces), so much less VdWr overlap is required at the same Y−X distance.

Implications of These Rsults on Conceptual Models of Molecular Geometry. Since this study sheds light on the physical forces that determine molecular geometry, it is fitting to use these results to assess the foundations on which the presently used conceptual models of molecular geometry are based.

(a) Hybridization (Directed Valence Theory). The results of this study **do not** support the core assumptions of hybridization. The bonding MOs generally show little sensitivity to geometry changes, and what sensitivity they do show is not in accord with the expectations of directed valence theory. In PH_3, for example, the bonding orbitals do show an angular preference, but it is for a X−Y−X angle of 120°, hardly what one would expect if the bonding were accomplished through nearly pure p-orbitals![1,34] Of course, a suggestion that directed valence theory is not physically realistic is hardly novel.[10,17,27,33,35,36] Group theory, supported by experiment, clearly shows that the bonding orbitals in molecules with T_d symmetry (i.e. CH_4) must have a singly degenerate orbital and a triply degenerate set of orbitals, not the quadrulply degenerate set envisioned as the four sp^3-hybird orbitals.[27] The above are only two of many examples, illustrating that the directed-valence theory often gives an incorrect impression of the actual forces at work in a molecule. Future generations of chemical educators may wish to reconsider the appropriateness of teaching this model of chemical bonding to introductory chemistry students.

(b) VSEPR (Electron Domain Theory). Electron domain theory, which underlies VSEPR, is on much firmer theoretical footing than is directed valence.[33] The results of this study, for the molecules NH_3 and PH_3, support the VSEPR model in its present form. However, when the terminal atoms bear nonbonding electrons, such as in NF_3, PF_3, or PCl_3, some revision of the VSEPR model appears to be necessary. The original points-on-a-sphere conception of Gillespie and Nyholm[5,8] is in agreement with the model suggested above, but the identification of a point with a bonding pair is in error, at least when that bond terminates with a halogen atom. The interactions involving the nonbonding electrons on terminal atoms clearly outweigh the interactions involving the bonding electrons, and so the VSEPR "point" is not the bond, but the nonbonded radii of the halogen atom. Recently, Gillespie and Robinson stated, "The interactions that determine (molecular) geometry are not only those between the bond pairs and the lone pairs, as assumed in the VSEPR model, but between all the electrons on one ligand and those on another—in other words ligand−ligand interactions and the interaction of ligands with any lone pairs."[17] Thus, it appears that even the developer of the VSEPR model understands the need for revision of the model,[24] and this work serves to quantify the scope of the necessary revision. Further study is required to determine how other terminal groups, such as organic moieties, should be correctly included in a revised VSEPR model.

(c) Perturbation Theory (Second-Order Jahn−Teller Effect) Model. An earlier attempt to use molecular orbitals to explain the geometry of the YX_3 (and other) molecules was based on perturbation theory, and focused on the interaction between the HOMO and LUMO.[18] The essential argument in this model is that a smaller HOMO-LUMO energy gap will yield smaller equilibrium X−Y−X angles and a larger inversion barrier. Based on some semiempirical calculations at the CNDO/2 level, this model showed promise in explaining the geometry and inversion barrier trends in the YH_3 and possibly YF_3 molecules.[10,19,20] However, HF/6-31G* calculations (checked at the MP2/CC-PVTZ level) of the HOMO-LUMO energy gap in the planar YX_3 molecules (Table 2) do not show the correlation to equilibrium geometry anticipated by this model. Specifically, NCl_3 has a much *smaller* energy gap than NH_3 and NF_3, but NCl_3 has an observed bond angle significantly *larger* than NF_3 and insignificantly different from NH_3. In the case of the phosphines, PF_3 and PCl_3 have very similar energy gaps, which are both *smaller* than that of PH_3, yet the observed bond angles in PF_3 and PCl_3 are both significantly *larger* than that in PH_3 (and significantly different from each other). Given these results, it is clear that the HOMO-LUMO gap of the planar YX_3 molecules is not meaningfully correlated to the equilibrium geometries of these molecules. On the basis of the data in Figure 4, it appears that the perturbation theory model underestimates the energy change of the other (non-HOMO) filled MOs in the geometry change from pyramidal to planar.

(d) LCP Model. Given the highly linear trends in Figure 7, it is fair to say that the LCP model,[21−24] at least in its qualitative form, is in essential agreement with the results of this study. This model fell into disuse due to its inability to incorporate central atom nonbonding electrons into the model; 40 years later this remains a difficulty but newer tools, such as accurate MO calculations, make the problem much more tractable. Given the similarity between the LCP and VSEPR models, it is realistic to suggest that both could be accommodated in a single conceptual model of molecular geometry.[17,24]

(e) Core Orbitals and Non-VSEPR Molecules. The surprising sensitivity of the core orbitals to geometry changes suggests an explanation of the "non-VSEPR" geometries in the Group 2 dihydrides and difluorides, such as CaH_2. Bader, Gillespie, et al.[16] have previously implicated the core orbitals as the primary

(34) Corbridge, D. E. *Phosphorus, An outline of its Chemistry, Biochemistry and Technology*, 3rd ed.; Elsevier: Amsterdam, 1985.

(35) Levine, I. N. *Quantum Chemistry*, 3rd ed.; Allyn and Bacon: Boston, 1983.

(36) Cooper, D. L.; Cunningham, T. P.; Gerratt, J.; Karadakov, P. B.; Raimondi, M. *J. Am. Chem. Soc.* **1994**, *116*, 4414.

cause of the nonlinearity of these molecules; these results appear to support such a hypothesis. Furthermore, the model of spreading and contracting forces presented above suggests that the bent geometries of these Group 2 YX_2 molecules is simply the product of the same forces that determine the geometry of all simple molecules. This will be an area of continued work in this laboratory.

Closing Comments. The nonbonded-interaction model, where the observed molecular geometry is seen as a balance of spreading and contracting forces, appears to have significant potential to explain trends in molecular geometry that have proved difficult for the standard (VSEPR and hybridization) models. This model can be seen as a refinement of the traditional VSEPR model,[5−9,17,24] and was first envisioned by Bartell in the 1960s.[21−24] Modern ab initio techniques give verification that the nonbonded-interaction model provides a more accurate representation of the physical forces responsible for observed geometry than do the hybridization or traditional VSEPR models, at least for halides as terminal atoms. This model successfully explains the bond angle trends of the Group 15 trihydrides and trihalides, and the Group 2 dihydrides and dihalides will soon be studied.

Acknowledgment. The authors wish to thank L. Vieland (Chatham College) for helpful suggestions on this work. Additionally, the Cottrell College Science Award of the Research Corporation (Nos. CC4008 and CC4681) and the Summer Research Award (No. 98-05) of Saint Louis University are thanked for their support of various portions of this work.

Supporting Information Available: Data from refined-distance calculation on NH_3, PH_3, NF_3, PF_3, and PCl_3 and complete molecular orbital visualizations fot he YX3 molecules (PDF). This material is available free of charge via the Internet at http://pubs.acs.org.

JA003604B